APCVD of Dual Layer Transparent Conductive Oxides for Photovoltaic Applications

Heather M Yates[1*], Jeffrey M Gaskell[2], Michael E Thomson[1], David W Sheel[1,2], Benoit Delaup[3], Monica Morales-Masis[3]

[1]Materials and Physics Research Centre, Cockcroft Building, University of Salford, Manchester, M5 4WT, UK

[2]CVD Technologies Ltd, Cockcroft Building, University of Salford, M5 4WT, UK

[3] EPFL STI IMT PV-LAB, Rue de la Maladière 71B, Neuchâtel, CH-2000, Switzerland

*corresponding author: H.M.Yates@Salford.ac.uk, phone +44 (0)161 295 3115, fax +44 (0)161 295 5575

Abstract

We report the atmospheric pressure chemical vapour deposition (APCVD) of a dual layer transparent conductive oxide (TCO). This combines a fluorine doped tin oxide (FTO) base layer with a fluorine doped zinc oxide (FZO) top layer, where we seek to utilise the respective advantages of each material and the differences in their associated industrial deposition process technologies. Deposition of a 250 nm thick FZO layer on FTO was enough to develop features seen with FZO only layers. The crystallographic orientation determined by the FZO dopant concentration. Changes to the deposition parameters of the underlying FTO layer effected stack roughness and carrier concentration, and hence optical scattering and absorption. Photovoltaic cells have been fabricated using this TCO structure showing promising performance, with efficiencies as high as 10.21% compared to reference FTO only values of 9.02%.

The bulk of the coating was FTO, providing the majority of conductivity and the large surface features associated with this material, whilst keeping the overall cost low by

utilising the very fast growth rates achievable. The FTO was capped with a thinner FZO layer to provide a top surface suitable for wet chemical or plasma etching, allowing the surface morphology to be tuned for specific applications.

Keywords: zinc oxide; tin oxide; atmospheric pressure chemical vapour deposition; PV

1. Introduction

Transparent Conducting Oxides (TCO's) are widely used throughout industry and in particular in the production of solar cells where highly optically transparent and relatively low electrical resistance front contacts are needed [1]. The TCO properties are of high importance in the efficiency of the resulting PV cells. One of the major factors is the surface morphology, in which roughness and feature type play a key role [2,3].

In this paper we discuss the effects of deposition parameters and use of dual layer TCO's on surface morphology and hence the properties of the fabricated PV cells. We demonstrate a dual layer stack of fluorine doped zinc oxide (FZO) on top of fluorine doped tin oxide (FTO) grown by atmospheric pressure chemical vapour deposition (APCVD). This dual layer approach has been used previously for TCO deposition in order to utilise the strengths of the individual coatings to produce a better composite film. For example, both gallium doped zinc oxide [4] and fluorine doped tin oxide [5] have been used to improve the thermal resistance of indium tin oxide films without significant detriment to the performance of the ITO layer. Similarly, antimony doped tin oxide has been used to stabilise aluminium doped zinc oxide [6]. Depositing a dual layer stack of the same material but with different growth conditions has been used to allow a separation of the conductivity and the light

scattering elements of boron doped zinc oxide, allowing for optimisation of both properties [7].

Fluorine doped tin oxide and doped zinc oxide films are both used extensively as TCOs in the production of photovoltaic devices. Each material has its own benefits and drawbacks. FTO films tend to be rougher than zinc oxide films and are cheaper to produce due to faster growth rates. The deposition of this material is well known due to its use in Low E coatings. However, it is susceptible to degradation from the hydrogen plasma used in the production of amorphous silicon and tandem silicon cells [8]. This in turn leads to reduced cell efficiency due to the poorer interface between the FTO and the silicon absorber, along with much reduced light transmission [9]. Zinc oxide based TCOs are often produced using low pressure techniques such as LPCVD which has an advantage of lower deposition temperatures than APCVD, although much slower deposition rates. However, they can be more easily etched than FTO to allow for modification of the surface structure. They are also more resilient to the amorphous silicon production process.

The goal of this work is to combine the strengths of FTO and FZO to produce a high-performance transparent conductive oxide. The FTO provided the majority of the conductivity and has the potential to reduce the overall cost of production, whilst the FZO layer can make the stack more controllable for surface structure, and at the same time protects the FTO layer from reducing during the H_2 plasma treatment used for the solar cell fabrication.

2. Experimental Details

2.1 TCO Growth

Fluorine doped zinc oxide was deposited from a precursor mixture of diethyl zinc, ethanol and trifluoroethanol (See Table 1). Diethyl zinc (DEZ) was selected as the zinc precursor due to its reactivity and high vapour pressure at low temperatures. Ethanol was used as an oxidant and trifluoroethanol was used as the fluorine source. The two liquids were mixed together in the appropriate ratio for the required film.

Fluorine doped tin oxide was deposited from a precursor mixture of monobutyltintrichloride (MBTC), oxygen, water and trifluoroacetic acid (TFA). MBTC was heated to 125°C in a stainless steel bubbler and introduced to the CVD reactor in a nitrogen gas carrier flow. Water and TFA were mixed to the appropriate ratio for the experiment and introduced to the CVD reactor by flash evaporation in a nitrogen carrier gas flow.

The FTO layer was deposited on a 1mm boroaluminosilicate glass substrate before being transferred to a different coater for the subsequent FZO deposition. Both layers were deposited using a lab-scale APCVD coater. The coating head was a 100mm wide ‘dual flow’ style design with a central inlet slot to make a uniform flow of reactive gases and two exhaust slots for drawing away the waste gases. The heated substrate was translated underneath the coating head for enough passes to build up the desired thickness of coating.

2.2 Cell fabrication

The a-Si:H/μc-Si:H micromorph tandem cells were deposited onto the FTO/FZO substrates (Fig.1). The micromorph cells consist of an a-Si:H top cell (210 nm) and a μc-Si:H bottom cell (1.25 μm). A SiO_x intermediate reflector layer was used in between the two subcells. All the layers were deposited by plasma enhanced chemical

vapour deposition (PECVD). A ZnO back electrode was deposited by low pressure CVD (LPCVD). The micromorph cell size was 1 cm^2.

2.3 Characterisation

The crystallinity and structure of the samples were assessed by X-ray diffraction (XRD) performed with a Siemens D5000 using a Cu Kα source. The morphology and surface roughness of the samples were obtained by atomic force microscopy (NanoScope IIIa, Digital Inst. Ltd.). Images were also obtained via scanning electron microscopy (FEI Quanta 250 ESEM) and by airSEM (beam energy 30kV, probe current 250pA). Film thickness was determined by etching the films with HCl/Zn metal to give a step edge, followed by surface profiling on a Dektak 3ST. The resistivity of the films was measured using a Jandel Universal four point probe. An Ecopia Hall effect measurement setup (HMS5000) was used to determine resistivity, Hall mobility and charge carrier density in the Van der Pauw configuration at room temperature. In order to determine the optical transmittance and the haze factor of the layers, spectrophotometry (UV-Vis-NIR) was performed with a Perkin-Elmer Lambda 900 spectrophotometer equipped with an integrating sphere.

For characterisation of the solar cells, current-voltage (I-V) and external quantum efficiency (EQE) were performed under AM1.5G-spectrum illumination and at room temperature. The short circuit current density (J_{sc}) values from the EQE measurements were used to calculate accurate cell efficiencies.

3. Results and discussion

This section is divided into two main parts. Firstly, the effects of varying the APCVD deposition parameters on the properties of the dual layer TCO thin film are discussed

(set 1) and the importance of these initial results on the solar cell are described. Secondly, based on these results a new set of samples (set 2) is discussed followed by final conclusions on these PV cells.

3.1 TCO Film Deposition

The FTO crystal facets acted as a new nucleation site for FZO deposition as either needles or plates, dependent on the dopant concentration. As the film thickness increased, a coherent FZO film developed. The morphology type was strongly dependent on the level of dopant in the FZO layer and will be discussed further in this paper (see section 3.11). Cross-sectional SEM (Fig.2) showed that the growth mechanism did not produce any noticeable voids or vacancies in the interface between the two films. The conductivity of the dual layer films was similar to that of an uncoated FTO layer of the same total thickness even with very low dopant concentrations in the FZO layer.

The calculated equivalent static deposition rates of the 2-layer structure were 5.5 nm/s for ZnO:F and 14-16 nm/s for FTO giving a weighted average of around 13 nm/s in comparison to the deposition rate of ZnO under LPCVD of approximately 4 nm/s. This improvement in deposition rate could possibly reduce commercial production costs.

3.11 Effect of FZO Dopant Concentration on Surface Structure

Deposition of FZO directly on glass substrates showed that low dopant concentrations tended to be almost exclusively (002) orientation, while high dopant concentration produced films with a mixed texture with (101) being more dominant. Deposition of films on FTO at all dopant levels produced films which contained both (101) and

(002) orientations. As the film thickness increased for the lower dopant films the (101) reduced and the (002) became more dominant so giving rise to a plate-like surface structure. In contrast films deposited on FTO at high dopant levels produced films in which initially the (002) dominated, but on increasing thickness a needle-like structure relating to the (101) phase of the hexagonal wurtzite structure (Fig.3) became more prominent.

In the example airSEM images (Fig.4) FZO deposited with over 30 mol% trifluoroethanol in the gas mixture exhibited a needle-like surface structure due to a preferred orientation for the (101) phase. Decreasing the percentage of dopant to below 5 mol% changed the preferred orientation of the FZO film to the (002) orientation, producing a plate-like structure. It can also be seen that 250 nm of FZO is enough for the coating to develop the features expected from a FZO only coating, rather than that of FTO only (fig.4a).

Films of FZO on glass are generally smooth with for example roughness (RMS) values under 10 nm for films around 300 nm thick. By depositing on FTO the surface roughness was increased. As can be seen in Table 2 the surface roughness of the dual layer stack could be tuned by varying the level of dopant in the FZO layer. Films with the (002) orientation had a significantly rougher surface than the (101) orientation, resulting in an overall increase in optical haze, which in turn should improve the current density obtainable in the PV cells. Previous work on F-doping another TCO, SnO_2, showed that increasing the dopant level reduced surface feature size and reduced roughness, with no change in orientation preference [10]. A similar change was seen by Elangovan et al [11] between undoped to doped SnO_2. These suggest that

the increased roughness seen here on increased doping level relates to the marked change in crystallographic orientation.

When FZO was deposited directly onto a glass substrate, the reduction in the amount of dopant led to a corresponding decrease in the conductivity of the film. However, with dual-layer stacks the conductivity of the film was dependent mostly on the bulk FTO layer. For example halving the amount of precursor TFA dopant in the FTO layer (0.2M to 0.1M) led to approximately 40% increases in sheet resistance. All other deposition conditions and individual layer thicknesses were identical. A 1000nm FTO/FZO stack has approximately an equivalent resistivity to that of a 1000nm FTO only layer. Hall data for the samples shows that the dual layer samples have a lower carrier concentration than that of the FTO layer, but the mobility is similar. The reduction in carrier concentration could be beneficial for certain applications such as amorphous silicon solar cells due to the reduction of the overall free carrier absorption of the stack [12].

3.12 Effect of layer thickness on roughness

The thickness of both the FZO and the FTO layer had a significant effect on the surface roughness of the dual layer stack (Fig.5). Increasing the thickness of FZO layer whilst keeping the thickness of the FTO layer the same, resulted in an increase in RMS from 26 to 55nm. However, FZO films thicker than 500 nm tended to crack and degrade over time. Increasing the thickness of the FTO layer whilst keeping the FZO layer the same, increased the roughness of the overall stack, but to a lesser extent than changing the FZO layer. If the thickness of the total stack was kept static at 1000nm, increasing the thickness of FZO whilst decreasing the thickness of FTO produced films with a greater RMS roughness.

3.2 Cell Results (set 1)

Taking the above results into consideration an initial set of dual layer FTO/FZO stacks were used in the construction of silicon micromorph cells. All FZO samples were deposited using a moderately high oxidant ratio (20:1) with the minimum FTO thickness and maximum FZO thickness to achieve high roughness levels, while reducing the possibility of cracking. An oxidant:zinc precursor ratio of 20:1 was chosen as a compromise between decreasing conductivity and increasing surface roughness due to an increasing preference for the (002) plane in the XRD. These in turn suggested the increased oxidant ratio reduced the level of doping in the film [13].

High and low F-dopant levels FZO films on FTO/glass were chosen for comparison. In addition two different quality Zn precursors were used. A high semiconductor grade dimethylzinc triethylamine adduct (SAFC) and standard grade DEZ (Aldrich) was used. The adduct is guaranteed free of metal impurities. An array of 10x10mm cells were deposited on a series of different stacks and the cell properties were measured. The results (Table 3) were compared to APCVD FTO-only coatings produced in our labs of a similar thickness and conductivity.

The dual layer samples all showed efficiencies greater than that of the control FTO only sample. The highest efficiencies were those with the lower doping level, FTO2-FZO20 and FTO2-FZO5, at 9.90% and 10.23% respectively. In general, the dual layer samples exhibited lower short circuit currents than the control FTO sample. As the short-circuit current is governed by the generation and collection of light-generated carriers, this was most likely due to the surface of the dual layer samples

giving less scatter than FTO only coatings, as reflected in the roughness values. However, both fill factor and V_{oc} were higher in the dual layer samples than the FTO standard. This increased the overall efficiency of the dual layer samples to greater than that of the control single layer FTO.

Sample FTO2-FZO16 has an identical stacked structure to FTO2-FZO20 except it has a highly doped F.ZnO layer. This produced a smoother surface with smaller, needle-like structures. The extra dopant would also increase the free carrier absorption of the FZO layer. These differences were reflected in the short circuit current, I_{SC}, of the cells. Although the best cell for FTO2-FZO16 listed in the table above is comparable to the other samples, its average result (4 cells) for short circuit current is 7.10 mA/cm^2, hence reducing overall efficiency.

A comparison of both low doped ZnO stacks shows only small differences between most of the cell data, although a higher efficiency was shown for the samples deposited used the high grade zinc adduct. This probably relates to increased impurities in the deposited layers for samples deposited using the lower grade precursor. However, the efficiency difference is acceptable (for research purposes), when balanced with the considerable difference in precursor cost.

These findings suggest that a lower dopant level in the FZO layer is preferable for better cell efficiencies due to reduced free carrier absorption and the creation of rougher surfaces due to the change in crystallographic orientation preferences.

3.3 TCO properties for set 2

A second sample set was deposited, with the aim to increase the roughness of the samples in order to improve scatter and enhance the cell short circuit current. This was achieved in two ways. Firstly, the amount of dopant in the FZO layer was decreased further as this had been found to substantially increase surface roughness (see Table 2) and thickness set to 280 nm. Secondly, a number of changes were made to the FTO layer to increase the roughness of the overall stack and decrease free carrier absorption. These are described in Table 4. The modified FTO deposition parameters were F-dopant levels, film thickness and water to MBTC ratio. The latter has been previously been found to have an effect on surface roughness [14].

Decreasing the amount of dopant in the FTO layer increased the sheet resistance of the overall stack. To keep the overall resistivity low the thickness of the FTO layer increased. This had the advantage of increasing the roughness of the dual layer stack surface, which in turn led to an average increase in optical haze (between 400 nm and 800 nm) from 10% to over 16%.

Reducing the amount of dopant in the FTO layer led to a decrease in the carrier concentration. This resulted in a reduction in absorption in the visible and near IR region as seen in Fig.6. This is likely due to the reduction of free carriers in the material. A similar trend was seen by Kim et al [15] for their pulsed laser deposited FTO of reduced transmission (increased absorption) on increasing the F-doping concentration. The reduced absorption seen for this work is extremely beneficial for solar cell applications due to the increase in light reaching the absorber.

The roughness (RMS) of all samples was greatly increased over that of the previous sample set, which should increase the scatter properties of the films. This should, in turn, increase the short circuit current. The surface roughness of all the dual layer samples is greater than FTO-only films of a similar thickness. The AFMs showed the surface structure is the plate-like structure associated with (002) zinc oxide films. This was mirrored by haze measurements of two samples FTO2-FZO20 (from set 1) and FTO2-FZO24 (set 2). The only difference between these two samples is the FZO layer, which has increased roughness on FTO2-FZO24, which led to a marked increase in haze at 450 nm from 6% to 14%.

Prior to fabrication of PV cells the Hall mobility and free carrier concentration for all the samples was tested (Table 5). Addition of the ZnO layer (FZO24) to the FTO (FTO1) changed the electrical properties of the film. Reduction of the level of dopant, while keeping reactant ratios constant also reduced the carrier concentration and hence optical absorption. Increasing the FTO layer thickness (FTO6 to FTO7) showed the expected reduction in sheet resistance, increased roughness and hence optical haze, although a small decrease in transmission. The final change in APCVD parameter was to reduce the water to tin precursor ratio from 20:1 to 10:1 (FTO9), while keeping the dopant level constant at 0.1 M. Despite having an overall thinner stack FTO9 showed comparable electrical properties to those of FTO7, with the exception of a lower mobility. Although FTO9 is thinner than the other samples it showed an increase in film roughness (as seen previously) which related to an improved optical haze.

3.4 Cell measurements for set 2

As before, micromorph tandem cells were fabricated and the results for the best cells are seen in Table 6. It can be seen that the standard FTO sample used for comparison,

despite being identical to the standard used for the first cell set gives slightly low cell efficiency. This is due to possible small changes in FTO production and cell fabrication, confirming the importance of fabrication of comparison standards concurrent to production of those on our dual layer TCO samples.

Reducing the dopant to very low levels in the FTO layer had a significant effect on improving cell efficiency (FTO13-FZO24) due to a decrease in the free carrier absorption (lower carrier concentration) and increased optical haze. The corresponding increased thickness to keep resistivity low does not seem to have had a large negative effect on the results, although it will have reduced transmission (over a thinner identical sample) and hence an effect on efficiency.

Higher efficiency was also seen when the water to tin precursor ratio was reduced (FTO9) compared to samples with identical doping levels (FTO6, 7), although thicker. FTO9 has the advantage of similar roughness to PLT7, although much thinner and hence improved transmission, which is reflected in the cell results.

The one very poor result was for FTO12-FZO24 which was surprising as the electrical and optical properties were not at the extremes of the range of values. Possibly there were problems with contacts for the I-V or EQE measurements.
In general, the dual layer samples exhibited lower open circuit voltage (V_{oc}) than the control FTO sample PLT 1. The short circuit current density (J_{sc}) was higher for the dual layers (especially in the bottom cell), which could be explained by the slight increase in surface roughness. The predominant factor for high efficiency in the cells seems to be the roughness of dual layer surface (Fig.7).

Overall the higher efficiencies were produced for dual layers for FTO's with the lowest dopant concentration, reduced water to tin ratios and thicker layers. Efficiencies of 8.89% were obtained for the dual layers compared to that of the FTO reference at 8.99%.

The aim for set 2 samples was to find APCVD deposition parameters which improved optical scattering via increased surface roughness. This was achieved along with enhanced J_{sc}. The importance of surface roughness to improve light scattering and hence J_{sc} and finally cell efficiency was seen in figure 7 and Table 2. These confirmed an increased cell efficiency as J_{sc} (for both top and bottom cells) increased. Although there is improved J_{sc} there is also an adverse effect on V_{oc} and especially the fill factor. These are now lower than that of the cell fabricated for the reference FTO only sample, in reverse to that seen for set 1. This has led to a reduction in efficiency to that previously seen in set 1 relative to the reference cell.

The morphology of the TCO has previously been reported to induce defects in silicon absorber layers [16,17]. With increased roughness in our TCO layers there may be poorer interface integrity with the absorber layers and hence reduced quality of silicon deposition. This in turn effecting in particularly the fill factor and V_{oc} and leading to poorer cell efficiency.

Ideally a balance of conditions is required for high values of all these cell parameters. If the haze of the dual layer samples could be increased further (to increase J_{sc}) together with a surface valley smoothening for a better growth of the Si layers

(improve V_{oc} and fill factor), through techniques such as surface etching, there is the potential for the dual layer TCO to produce higher efficiency cells than FTO alone.

4. Conclusion

In this paper we have demonstrated the effects of APCVD deposition parameters on polycrystalline dual layer FTO/FZO films. An APCVD process can be defined for improved TCO structures consisting of dual SnO_2:F/ZnO:F layers, which has the possibility to reduce production costs via increased deposition rates over that of single layer FZO. These are potential candidates for PV improvement over that of single layer APCVD ZnO or FTO with the additional benefits of improved protection against H_2 plasma etching during the fabrication of PV cells and potential for reduced production costs. Initial micromorph cells from the 2-layered TCO showed efficiencies greater than that from the control single layer FTO deposited under conditions which had previously led to micromorph cells with efficiencies greater than that of high quality commercial on and off line products [11]. A further increase in efficency could be gained by use of high purity precursors.

Use of FTO capped films with a thinner FZO layer should provide a top surface which would be suitable for wet chemical or plasma etching [18], allowing the surface morphology to be tuned for specific applications.

5. Acknowledgements

We would like to thank B-Nano Ltd for the airSEM images and Salford Analytical Services for the cross-sectional SEM. This work was financed by Framework 7 grants FP7 NMP CP-IP 214134-2 N2P “Flexible production technologies and equipment based on atmospheric pressure plasma processing for 3D nano-structured

surfaces" and FP7 NMP.2012.1.4-1 309530 PLIANT "Process line implementation for applied surface nanotechnologies".

List of Figures and Tables

Fig.1, Thin film Si cell (pin configuration) and back contact depositions

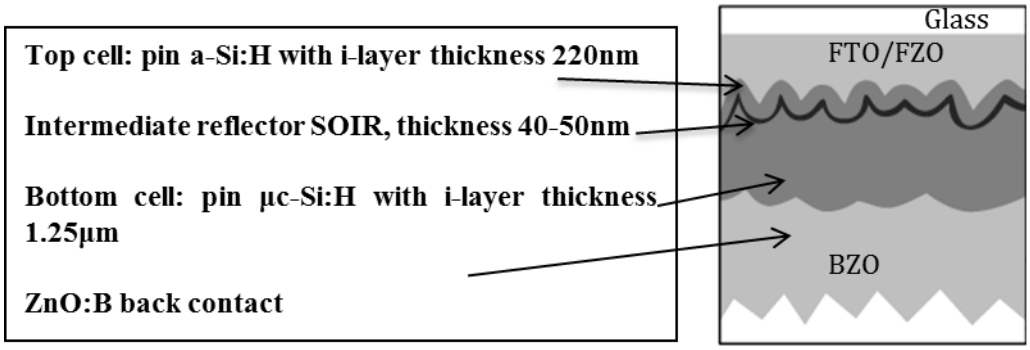

Fig.2, Cross-sectional SEM of a dual FTO-FZO film on glass.

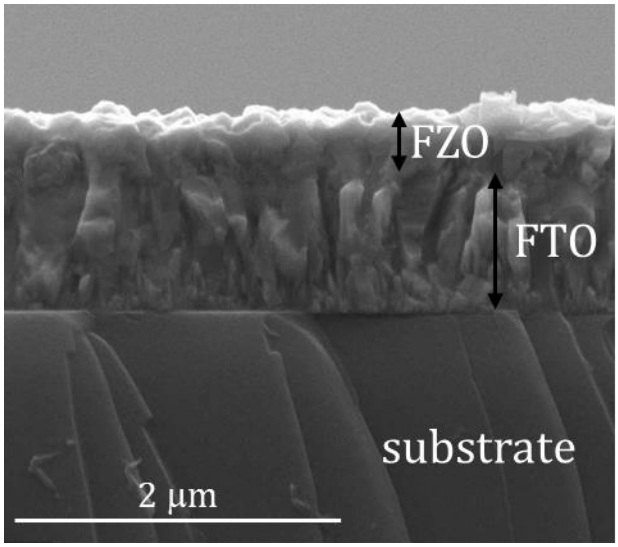

Fig.3, XRD (a) highly dopant FZO on glass, (b) highly dopant FZO on FTO, (c) low dopant FZO on glass, (d) low dopant FZO on FTO

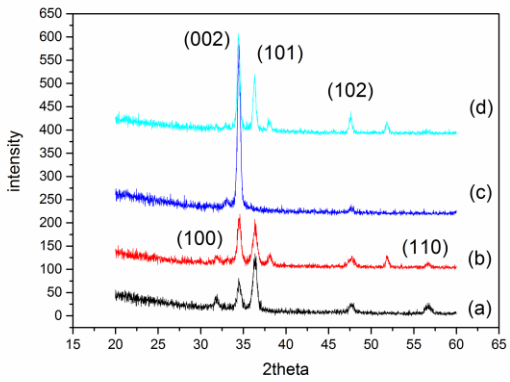

Fig.4, AirSEM images of (a) FTO base layer, (b) low dopant FZO on FTO, (c) high dopant FZO on FTO

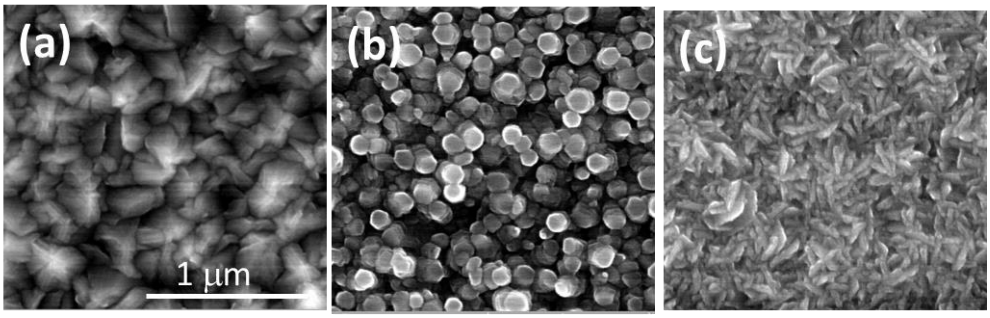

Fig.5, Effect of stack thickness on surface roughness.

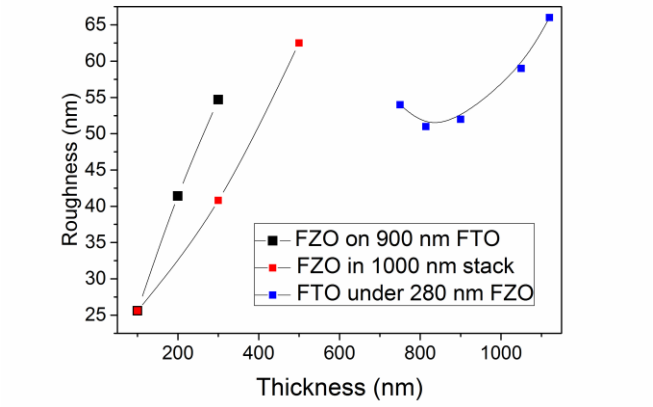

Fig.6, Graph of TFA precursor concentration against optical absorption at 800 nm and 1500 nm.

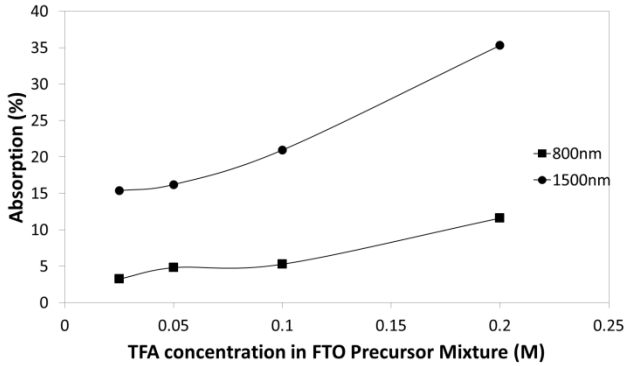

Fig.7, Graph of the overall efficiency of the cell against surface roughness of the dual layer stack.

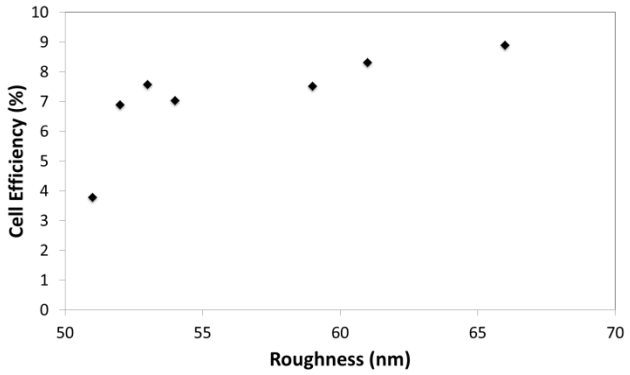

Table 1, APCVD deposition parameters

Parameter FTO	**Value**
Substrate Temperature	600°C
MBTC molar flux	$6.1x10^{-4}$ mol/min
TFA solution concentration	0.2-0.025M
Water:Tin precursor Ratio	20:1-10:1
Oxygen Flow Rate	1.4 l/min
Total Flow	7 l/min

Parameter FZO	**Value**
Substrate Temperature	410°C
DEZ molar flux	$5.5x10^{-4}$ mol/min
Ethanol:DEZ ratio	20:1
Molar percentage Tetrafluoroethanol	2.5-37%
Total Flow	6 l/min

Table 2, Dopant concentration against stack roughness and XRD orientation

Sample	TFE concentration	Preferred Orientation	Dual layer Roughness (nm)
FTO2/FZO16	37%	(101)≥(002)	19
FTO 2/FZO 20	3.1%	(002)>>(101)	28
FTO 6/FZO 24	2.5%	(002)	54

Table 3, Selected cell properties

samples	TCO Structural properties			Solar Cell properties			
	Structure FTO/FZO nm	Sheet Resistance Ω/sq	RMS nm	J_{sc} mA/cm^2	V_{OC} mV	FF %	Eff. %
FTO1 FTO only	1000/0	12	45	9.099	1305	75.6	9.02
FTO2+FZO16 FZO highly doped	750/250	12	19	7.491	1405	80.5	9.26
FTO2+FZO20 FZO low doping	750/250	13	28	8.248	1365	79.2	9.90
FTO2+ FZO5 FZO low doping, adduct	750/250	12.5	23	7.974	1394	79.9	10.23

Table 4, Summary of FTO layer changes

sample	APCVD parameters		Thickness nm		RMS roughness, nm	
	Water:MBTC	TFA Molar	FTO layer	total	FTO layer	FTO/FZO Stack
FTO1	20:1	0.2	1000	1000	45	N/A
FTO2	20:1	0.2	750	1030	30	53
FTO6	20:1	0.1	750	1030	19	54
FTO7	20:1	0.1	1050	1330	41	59
FTO9	10:1	0.1	600	880	39	61
FTO12	20:1	0.05	814	1094	44	51
FTO13	20:1	0.025	1120	1400	35	66

Table 5, Electrical measurements of the dual layer samples

	Hall effect measurements			
Sample	Bulk concentration (cm^{-3})	Resistivity (Ω.cm)	Mobility (cm^2/(V.s)	R_{sh} (Ω□)
FTO1	1.63E+20	9.22E-04	41.57	9.22
FTO2 FZO24	1.21E+20	1.21E-03	43.19	11.75
FTO6 FZO24	6.13E+19	2.43E-03	41.97	23.59
FTO7 FZO24	8.85E+19	1.54E-03	45.70	11.58
FTO9 FZO24	9.85E+19	1.60E-03	39.69	18.18
FTO12 FZO24	7.39E+19	2.01E-03	42.14	18.37
FTO13 FZO24	7.01E+19	2.59E-03	34.49	18.50

Samples	J_{sc} (mA/cm^2) Top cell	J_{sc} (mA/cm^2) Bottom cell	V_{OC} (mV)	FF (%)	Eff. (%)
FTO1	11.42	8.66	1338.0	77.55	8.99
FTO2+FZO24	11.77	10.22	1261.3	58.68	7.56
FTO6+FZO24	11.79	10.58	1220.2	54.48	7.03
FTO7+FZO24	11.82	10.50	1228.0	58.24	7.51
FTO9+FZO24	11.96	10.53	1277.5	61.73	8.30
FTO12+FZO24	9.32	8.44	1105.3	40.40	3.77
FTO13+FZO24	12.13	10.89	1246.8	65.44	8.89

Table 6, Cell results for the dual layer samples

6. References

[1] C. Beneking, B. Rech, S. Wieder, O. Kluth, H. Wagner, W. Frammelsberger, R. Geyer, P. Lechner, H. Rubel, H. Schade, Thin Solid Films 351 (1999) 241-246.

[2] J. Bailat, D. Dominé, R. Schlüchter, J. Steinhauser, S. Faÿ, F. Freitas, C. Bücher, L. Feitknecht, X. Niquille, T. Tschamer, A. Shah, C. Ballif, Proceedings of the IEEE World Conference on PV Energy Conversion, Waikoloa, HI, May 2006.

[3] J. Krc, B. Lipovsek, M. Bokalic, A. Campa, T. Oyama, M. Kambe, T. Matsui, H. Sai, M. Kondo, M. Topic, Thin Solid Films, 518 (2010) 3054-3058.

[4] A. Chung, S. Cho, W. Cheong, J.Ceram.Process. Res. 13 (2012) 10–15.

[5] T. Kawashima, T. Ezure, K. Okada, H. Matsui, K. Goto, N. Tanabe, J. Photochem. Photobiol.A. 164 (2004) 199–202.

[6] M. Cao, Y. Li, J. Yang, Y. Chen, Study for double-layered AZO/ATO transparent conducting thin film. J.Phys.Conf.Ser. 419 (2013) 012022.

[7] X. Zhang, Q. Huang, Y. Wang, Y. Liu, X. Chen, Y. Zhao, Thin Solid Films, 520 (2011) 1186–1191.

[8] H.N. Wanka, M.B. Schubert, E. Lotter, Sol.Energy Mater.Sol.Cells 41/42 (1996) 519-527.

[9] R. Das, T. Jana, S. Ray, Solar Energy Materials and Solar Cells, 86 (2005) 207-216.

[10] H.M. Yates, P. Evans, D.W. Sheel, Physics Procedia, 46 (2013) 159-166.

[11] E. Elangovan, K. Ramamurthi, Thin Solid Films, 476 (2005) 231-236.

[12] G.J. Exarhos, X.-D. Zhou, Thin Solid Films, 515 (2007) 7025–7052.

[13] M.Thomson, 'The Modification of Thin Film Surface Structure via Low Temperature Atmospheric Pressure CVD Post Process Treatment', PhD Thesis, University of Salford, 2014.

[14] H.M. Yates, P. Evans, D.W. Sheel, S. Nicolay, L. Ding, C. Ballif, Surf.Coat.Technol. 213 (2012) 167-174.

[15] H. Kim, R.C.Y. Auyeung, A. Piqué, Thin Solid Films, 516 (2008) 5052-5056.

[16] D. Knoesen, R.E.I. Schropp, W.F. Van der Weg, Proc. Mat. Res. Soc. Symp 377 (1995) 597.

[17] G. Bugnon, G. Parascandolo, T. Söderström, P. Cuony, M. Despeisse, S. Hänni, J. Holovský, F. Meillaud, C. Ballif, Adv. Funct. Mater. 22 (2012) 3665.

[18] M.Thomson, J.L. Hodgkinson, D.W. Sheel, Surf.Coat.Technol. 230 (2013) 190-195.